Federal University of Ouro Preto, Minas Gerais, Brazil

Intra-articular leflunomide-loaded poly(ε-caprolactone) implants to treat synovitis in rheumatoid arthritis

T. F. Gomes, F. C. M. Gualberto, F. B. Perasoli, F. P. Andrade, S.A. L. Moura, G. R. Da Silva*

Received November 22, 2018, accepted January 14, 2019

**Corresponding author: Gisele Rodrigues Da Silva, Federal University of Ouro Preto, Morro do Cruzeiro w/n, Bauxita, Ouro Preto, Minas Gerais, 35400-000, Brazil.*
giselersilva@ufop.edu.br

Pharmazie 74: 212-220 (2019) *doi: 10.1691/ph.2019.8223*

Rheumatoid arthritis is an autoimmune pathology that manifests as chronic inflammatory arthropathy and synovitis. Treatment of rheumatoid arthritis is based on the administration of different types of drugs, including leflunomide, an antirheumatic drug. However, the long-term systemic use of leflunomide may be associated with adverse effects. Local therapy could be an efficient strategy to treat synovitis triggered by rheumatoid arthritis without inducing adverse effects. In this study, leflunomide-loaded poly(ε-caprolactone) implants (leflunomide PCL implants) were evaluated as local drug delivery systems capable of attenuating inflammation and angiogenesis, which represent events of synovitis. Leflunomide PCL implants were designed by hot molding technique; and they were characterized by FTIR and DSC. These analytical techniques demonstrated the chemical integrity and dispersion of drug into the polymeric chains. Then, a spectrophometric method was developed and validated to quantify the leflunomide incorporated into the PCL implants and released from them. Linearity was obtained by ordinary least squares regression method to estimate the linear regression equation. Residues were evaluated considering normality, independence and homoscedasticity. Precision was lower than 5 %, and accuracy ranged from 98 to 104.5 %. Quantitation limit was 2.0 μg mL^{-1}. PCL implants provided controlled and sustained release of leflunomide for 30 consecutive days after inserting these systems in the subcutaneous tissue of mice. The main mechanisms of drug delivery were solubilization and diffusion from polymer. Then, a non-biocompatible sponge was inserted into the subcutaneous tissue of mice to function as a frame to develop the inflammatory and angiogenic processes. Leflunomide PCL implants were inserted in direct contact with the sponge. At 4, 7 and 10 days after-sponge implantation, the key components of inflammatory angiogenesis were measured to verify the regression of these events induced by drug. Leflunomide controlled released from polymeric implants downregulated the neutrophil and monocyte/macrophage infiltration due to the reduced expression of myeloperoxidase (MPO) and *N*-acetyl-β-d-glucosaminidase (NAG), respectively. As the influx of these pro-inflammatory cells was modulated by leflunomide, the production of nitric oxide (NO), a pro-inflammatory substance, reached low concentrations in the sponge. As a consequence of the modulation of inflammation at the pathological site, the angiogenic process was downregulated, since the hemoglobin levels in the sponge were drastically reduced. The accumulation of leflunomide in the pathological site did not induce nephrotoxicity or hepatototoxicity, as confirmed by histological analyses. Finally, intra-articular leflunomide PCL implants represent a potential therapeutic alternative to treat locally the synovitis triggered by rheumatoid arthritis without inducing systemic adverse effects.

1. Introduction

Rheumatoid arthritis is a systemic autoimmune disease that affects the synovial membrane, a thin layer of connective tissue that works as a coating of articular structures (Hernádez et al. 2014). Persistent synovitis leads to cartilage destruction, bone erosion and periarticular decalcification resulting in impaired joint function, motor disabilities and systemic complications. As a consequence of these outcomes, pain becomes the major symptom for patients with rheumatoid arthritis compromising their quality of life (Scott et al. 2010; Siafaka et al. 2016). Current therapeutic options include disease-modifying antirheumatic drugs (DMARDs) (Bastian et al 2011; Boone et al. 2015) such as leflunomide, a drug that has been shown to be effective in modulating the inflammatory response inrheumatoid arthritis (Siafaka et al. 2016).

Leflunomide (N-[(4-trifluoromethyl) phenyl]-5-methylisoxazole-4-carboxamide) is a synthetic derivative of isoxazole, endowed with immunomodulatory and anti-inflammatory characteristics, and licensed for treatment of rheumatoid arthritis (Day 2008). Its prolonged use is associated with serious adverse events, being the most significant the liver damage, myelosuppression and heart attack (Xuan et al. 2018; Alén et al. 2018; Rubinstein et al. 2012; Mcinnes et al. 2010; Bongartz et al. 2006). In 2010, the FDA added a warning on the drug labels on the risk of severe hepatic leflunomide injury based on a review that identified 49 cases of severe liver damage, including 14 cases of fatal liver failure in the previous seven years (U.S. FDA 2010).

Local intra-articular implantable devices would provide the control of inflammation and immunossuppression directly in the target organ, limiting the systemic drug distribution, and consequently, reducing/inhibiting the systemic adverse events. A number of studies have shown the efficacy of these polymeric implantable devices in modulating the inflammatory and immune responses and in suppressing systemic side effects in a murine model of inflammatory angiogenesis. In this experimental model, non-biocompatible polymeric sponges, subcutaneously inserted in mice, act as a frame for locally inducing infiltration, proliferation, and activation of inflammatory cells that induce the neovascularization and extracellular matrix deposition, leading to acute and chronic inflammation (Orellano et al. 2015).

Oliveira et al. (2018) have demonstrated that tacrolimus delivered from poly(ε-caprolactone) (PCL) implants suppressed inflammation and angiogenesis induced by non-biocompatible polymeric sponges. In addition, tacrolimus controlled and prolonged released from implants in the pathological site did not induce hepatotoxicity, nephrotoxicity and myelosuppression. Moura et al. (2011) have developed implants based on biocompatible and biodegradable polyurethane and dexamethasone capable of locally eliminating the inflammatory and angiogenic processes in this murine model of inflammatory angiogenesis. Finally, Oliveira et al. (2015) have explored the capability of methotrexate controlled released from PCL implantable devices in decreasing the recruitment and influx of inflammatory cells, blood vessel formation, cytokine release and extracellular matrix deposition in a murine model of inflammation and angiogenesis. Moreover, this *in vivo* model permitted to investigate the inability of the methotrexate locally released from polymeric implants in inducing severe systemic adverse effects, including nephrotoxicity, hepatotoxicity and an adverse hematopoietic profile.

In this study, leflunomide PCL implants were developed, and their efficacy in modulating the inflammatory and angiogenic responses in a murine sponge model was investigated. Firstly, these implantable devices were characterized by different analytical techniques including FTIR and DSC to verify the inexistence of a chemical interaction between drug and polymer. The lefluomide released from PCL implants was quantified for a long period to demonstrate that therapeutic doses of leflunomide could be delivered by these systems in a controlled and sustained way. To quantify the leached drug, a spectrophotometric method was developed and validated considering the following parameters: linearity, precision, accuracy and quantitation limits. Finally, leflunomide PCL implants were inserted into the subcutaneous tissue of mice which previously received non-biocompatible sponges to establish the inflammation and angiogenic processes. The leflunomide continuosly released from polymeric implants modulated the expression of myeoloperoxidase (MPO) and *N*-acetyl-β-d-gluocosaminidase (NAG), indicating that the levels of neutrophils and monocyte/macrophage, respectively, in the pathological site were downregulated by the implantable devices for ten consecutive days. This drug also reduced the accumulation of nitric oxide (NO) in the sponge frame; as well as the production of hemoglobin (Hb), inhibiting angiogenesis. Therefore, it was hypothesized that leflunomide-loaded PCL implants could attenuate the progressive joint damage in the rheumatoid arthritis, by controlling synovitis, neovascularization and immunological components locally established in joints in rheumatoid arthritis patients.

2. Investigations, results and discussion

2.1. Development of leflunomide PCL implants

Leflunomide PCL implants were prepared by the hot molding technique. Drug and polymer were solubilized in acetonitrile to provide a molecular mixture of compounds. Then, the organic solvent was evaporated, and the blend was molded under heating at approximately 60-70 °C. This temperature range induces polymeric fusion, which propitiates the entrapment of leflunomide into the polymeric chains. Implants were designed as flat spheres measuring 4.98±0.07 mm in diameter, 0.65±0.03 mm in thickness, and 9.94±0.07 mg in average weight (n = 10). Leflunomide content into PCL implants was 99.97±2.10 % (n = 10). The obtained value indicated that leflunomide was uniformely distributed within the implants. It has been previously reported that one possible disadvantage associated with the melting fabrication process of implants is the non-uniform dispersion of drugs in the polymeric matrix, due to a short time mixing of components (Cheng et al. 2009). However, the homogeneous distribution of leflunomide into the units and drug content close to the totality indicated that the manufacture method was suitable to obtain a good distribution of leflunomide in PCL implantable devices, without losing compound during manufacture.

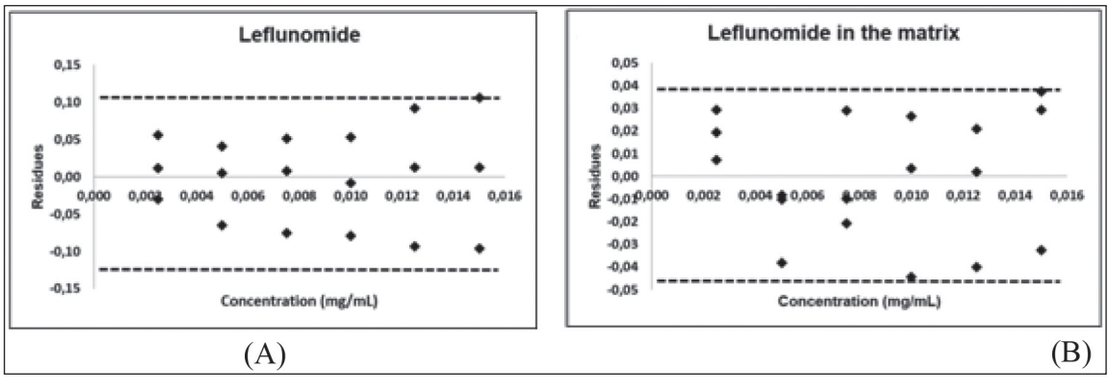

Fig. 1: Residual plots for outlier by Jacknife standardised residuals test. (A) leflunomide; (B) leflunomide in contact with PCL (matrix).

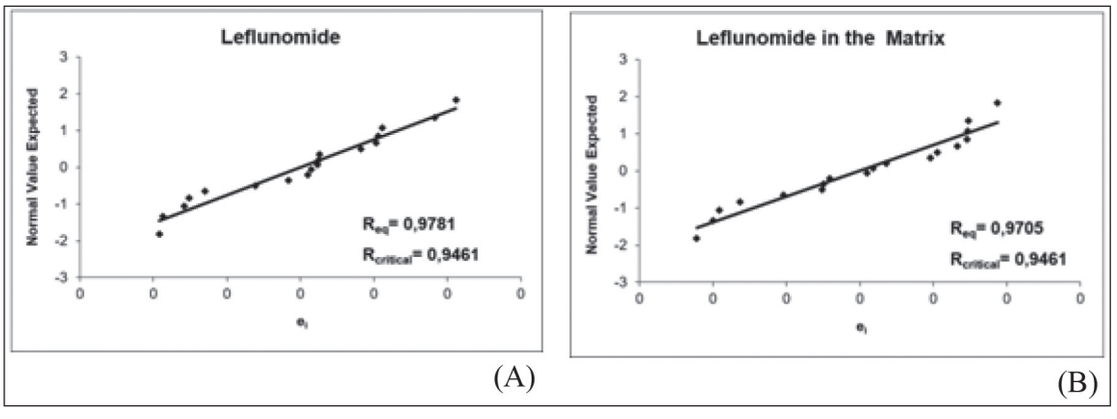

Fig. 2: Normal QQ plots of residuals for (A) leflunomide; and (B) leflunomide in contact with PCL (matrix).ei: residual. R: correlation coefficient of Ryan-Joiner test.

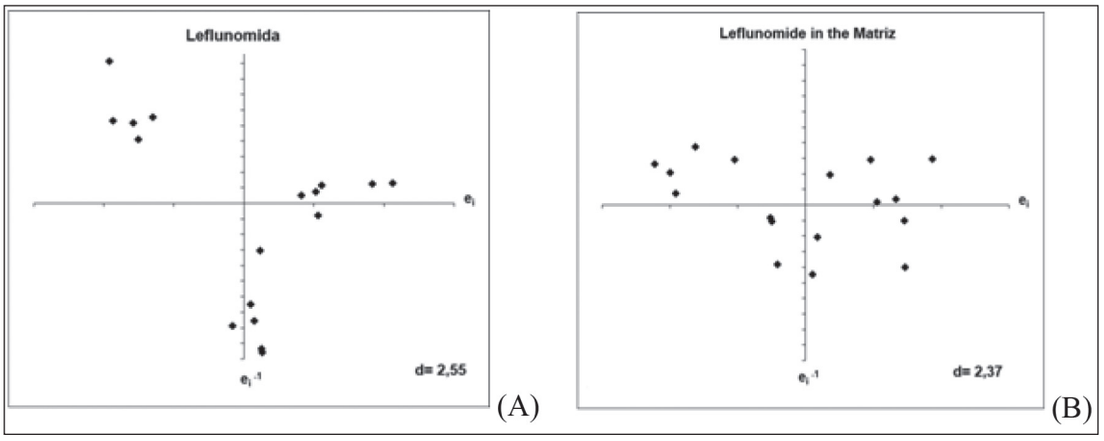

Fig. 3: Plots of residuals autocorrelation. (A) leflunomide; (B) leflunomide in contact with PCL (matrix).ei: residual. d: Durbin-Watson statistic.

Table 1: Residual homoscedasticity evaluation by modified Levene test

Statistic	Leflunomide	Leflunomide/matrix
t_L	1,33	0,949
dU	2.89	2.88

2.2. Method validation

Calibration curves of leflunomide and leflunomide in contact with PCL (matrix) were obtained from six drug concentrations (2.5; 5.0; 7.5; 10.0; 12.5 and 15.0 μg mL^{-1}) in three independent replicates, performed in random order. Figure 1 represents the graphs of residues (regression residues versus leflunomide concentration levels) for leflunomide in contact with PCL (matrix). Dotted lines correspond to $\pm t_{(1-\alpha/2;n-2)}$Sres, which is the acceptable variation range for regression residues (Silva et al. 2018). It can be observed that there were not outliers in the evaluated solutions. It indicates the absence of values that can influence the regression equation. Then, the assumption that residues followed the normal distribution was evaluated by Ryan-Joiner test. Figure 2 depicted the QQ plots, and their Ryan-Joiner correlation coefficients. It can be observed in this figure that there is a significant correlation between the two components (Req > Rcrit), indicating that there is no deviation from the normality when α = 0.10. According to the Durbin-Watson statistic, correlation residues (D = 2.55 > dU = 2.89 for leflunomide and D = 2.55 > dU = 2.88 for leflunomide in the matrix, both for α = 0.05) indicate independence of the residues. This homoscedastic behavior is also present on residues graphs (Fig. 3), where there is a random distribution of the residues. In addition, Table 1 shows that the residue variability of all drug concentrations was not significantly different (p > 0.05), indicating homoscedasticity (Souza et al. 2005; Silva et al. 2018).

After verifying the premises required by OLSM, the following regression equations were retrieved: Abs = 76.613 [leflunomide] + 0.0899 (R^2 = 0.9687) to the analytical blank and Abs = 77.025 [leflunomide] – 0.0188 (R^2 = 0.9937) to matrix solution (Fig. 4). The regressions for the two evaluated media were substantial for p < 0.05 (F > Fcrit = 4.49), Table 2. In this sense, the linearity of method for the two digested flours ranged from 2.5 to 15 μg mL^{-1}. Slopes and intercepts of calibration curves of leflunomide and leflunomide in contact with PCL (matrix effect) were compared using the Student's t-test in order to evaluate the possible interference of PCL in drug quantitation. This analysis indicated that slopes and intercepts from both calibration curves were not statistically different, showing that PCL did not interfere in quantifying leflunomide. Finally, the limit of quantitation, calculated by equation 1, was 2.0 μg mL^{-1} of leflunomide.

Data from intra-assay precision (repeatability) and inter-assay precision (intermediate) tests were expressed as coefficient of variation (CV); and they are summarized in Table 3. CV values were less than 5 % for all drug concentrations; thus indicating the precision of the spectrophotometric method. Data from accuracy tests indicated that leflunomide was recovered from the matrix in the range from 98.2 to 104.5 %, as shown in Table 3, demonstrating the accuracy of the method (Souza et al. 2005; Silva et al. 2018).

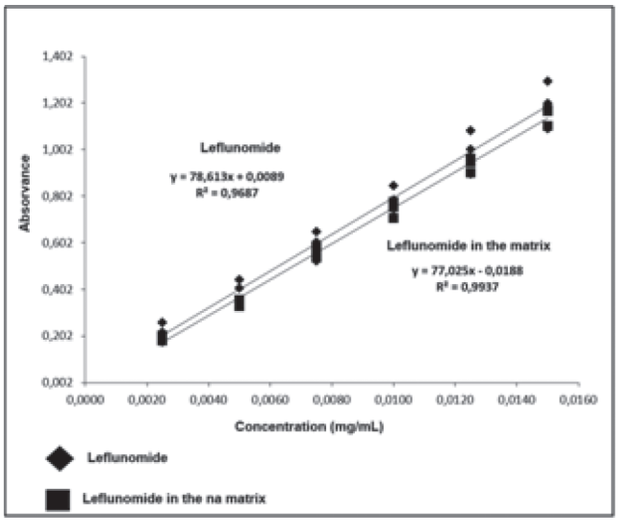

Fig. 4: Calibration curves of leflunomide, and leflunomide in contact with PCL (matrix). Regression equations and determination coefficients (R2) were expressed.

Table 2: ANOVA statistics for regression including lack-of-fit test

Source	d. f.	SS	MS	F	F critical	P
Leflunomide						
Due to regression	1	2.03	2.03	495.44	4.49	1.83×10^{-13}
Residual	12	6.55×10^{-2}	4.09×10^{-3}			
Lack-of-fit	4	1.25×10^{-3}	3.13×10^{-4}	0.059	3.25	9.93×10^{-1}
Pure error	8	6.42×10^{-2}	5.35×10^{-3}			
Total	13	2.09				
Leflunomide/Matrix						
Due to regression	1	1.95	1.95	2517.98	4.49	4.98×10^{-19}
Residual	16	1.24×10^{-2}	7.73×10^{-4}			
Lack-of-fit	4	2.67×10^{-3}	6.69×10^{-4}	0.828	3.25	5.33×10^{-1}
Pure error	12	9.70×10^{-3}	8.08×10^{-4}			
Total	17	1.96				

2.3. Characterization

2.3.1. FTIR

Figure 5 shows FTIR spectra of pure leflunomide (Fig. 5A), leflunomide PCL implants (Fig. 5B), and unloaded PCL implants

Table 3: Mean content of leflunomide in the intra-assay and inter-assay precisions and accuracy.

Level	5.0 µg mL-1 (50%)	1.0 µg mL-1 (100%)	15 µg mL-1 (150%)
Day 1	0.52 ± 0.00 (R = 103.3%; %CV = 0.04)	1.03 ± 0.00 (R = 103.2%; %CV = 0.1)	1.53 ± 0.00 (R = 101.7%; %CV = 0.1)
Day 2	0.50 ± 0.00 (R = 99.4%; %CV = 0.4)	0.98 ± 0.00 (R = 98.2%; %CV = 0.1)	1.48 ± 0.00 (R = 98.4%; %CV = 0.1)
Day 3	0.48 ± 0.00 (R = 104.5%; %CV = 0.3)	1.04 ± 0.00 (R = 103.6%; %CV = 0.1)	1.52 ± 0.02 (R = 101%; %CV = 1.1)
Precision Inter- assay (n= 9)	0.51 ± 0.01 (R = 102.4%; CV = 1.9)	1.02 ± 0.02 (R = 102.0%; CV = 2.3)	1.51 ± 0.02 (R = 100.4%; CV = 1.4)

(Fig. 5C). Typical infrared absorption bands observed in PCL were detected in spectra of Figs. 5B and 5C, such as at ~1700 cm^{-1} due to the carbonyl stretching vibration of ester groups; at 1166 cm^{-1} related to the C-O and C-C stretching in the amorphous phase; at ~ 2860 cm^{-1} and ~ 2940 cm^{-1} equivalent to symmetric and assymetric CH_2 stretching, respectively. These FTIR results corroborated with those previously described (Belsley et al. 1980). FTIR spectrum revealed characteristic absorption bands of leflunomide (Figs. 5A and 5B, Horwitz 1995): at ~1310 cm^{-1} due to the C-F; at ~1600 - 1700 cm^{-1} related to C=O stretching vibration; at 3300 - 3100 cm^{-1} corresponding to the hydrogen stretching vibration of amine. Therefore, the IR spectrum of leflunomide PCL implants showed all bands of characteristic organic groups of drug and polymer. In addition, new bands for drug-loaded PCL implants were not detected. All these findings show that chemical interactions between compounds or functional organic group modifications were not detected even after the manufacturing process of implants.

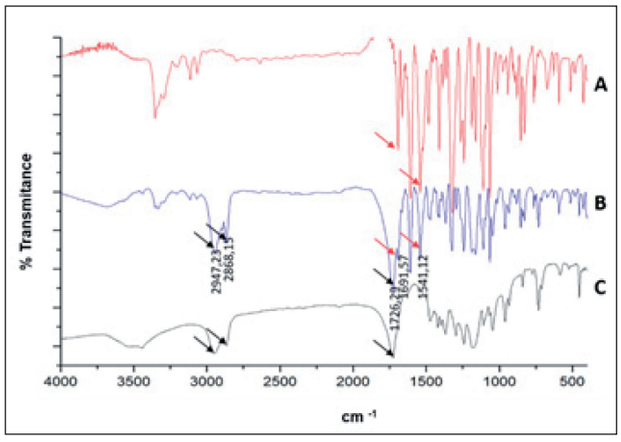

Fig. 5: FTIR spectrum of leflunomide (A), leflunomide PCL implants (B), and PCL implants (C).

2.3.2. DSC

Figure 6 represents DSC thermograms of leflunomide (Fig. 6A), PCL implants (Fig. 6B), and leflunomide PCL implants (Fig. 6C). The DSC curve of leflunomide indicated an endothermic event at 168.2 °C equivalent to its melting point. In addition, an endothermic event at approximately 260 °C was identified, representing the degradation of leflunomide (Vega et al. 2006). Therefore, thermal stability of leflunomide was preserved during the hot molding technique of implants, since the temperature of manufacturing was 60 – 70 °C. The DSC curve of unloaded PCL implants (Fig. 6B) indicated the melting of a polymeric crystalline phase at 63.7 °C. Finally, DSC the thermogram of leflunomide PCL implants showed a unique endothermic peak at 59.4 °C, corresponding to the melting of PCL. The absence of endothermic events of leflunomide was related to the fact that this drug was completely dispersed in the polymeric chains in an amorphous structure. According to Mccauley et al. (2005), the suppression of thermal events of drug incorporated into a polymeric system indicates the formation of a binary amorphous dispersion. Therefore, the incorporation of leflunomide as an amorphous structure into the polymeric chains was attributed to its dispersion rather than molecular interactions, which were not detected in FTIR results.

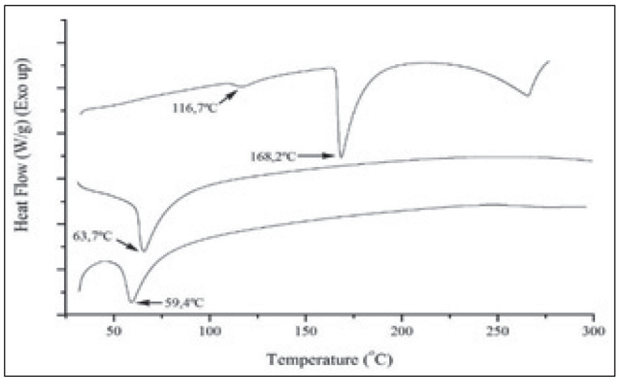

Fig. 6: DSC thermograms of leflunomide (A), PCL implants (B), and leflunomide PCL implants (C).

2.4. *In vitro release of leflunomide from PCL implants*

Figure 7 shows the *in vitro* release profile of leflunomide from PCL implants over a period of 90 consecutive days. PCL implants led to a controlled and sustained release of leflunomide, since approximately 40 % of the drug was leached from the devices during the study period. In addition, the pattern of drug release from implants was composed of two distinct stages. During the first 7-day period, the polymeric devices released an initial burst of drug corresponding to 12 %. The existence of the burst effect of drug

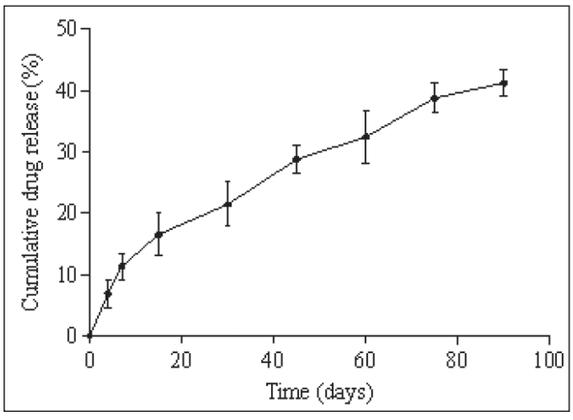

Fig. 7: In vitro cumulative release of leflunomide (%) from PCL implants. Results represent mean ± standard deviation ((n = 5 for each day).

indicated the presence of leflunomide at the surface of implantable devices, leading to the rapid drug solubilization and diffusion. In the second stage, which occurred between the 8th and the 90th day of the test, approximately 28 % of leflunomide was delivered from implants, demonstrating a long period of controlled and sustained release of this drug entrapped into the polymeric chains of PCL. At this moment, the water uptake induced the dissolution of leflunomide dispersed in the polymer; and the PCL delivered the drug in a slow rate during the days. Furthermore, the hydrophobic character of PCL and leflunomide induced the controlled delivery of drug from implantable devices. Diffusion was the main mechanism of leflunomide release from the polymeric implants, since the PCL presents an extremely slow biodegradation rate, which can be extended over a prolonged period of at least one year (Solano et al. 2013); therefore, polymeric erosion did not contribute to the mechanism of leflunomide delivery.

2.5. In vivo release of leflunomide from PCL implants

Polymeric implants provided a controlled and sustained release of leflunomide over a 30-day period within the subcutaneous tissue of mice (Fig. 8). PCL implants exhibited an initial burst release, since approximately 15 % of leflunomide was released during the first 7 days of the test. Afterwards, from the 8th and the 30th day, the rate of drug release markedly decreased. During this period, 9.8 % of the leflunomide was leached from the implantable devices. An average daily release of 16.51 ± 2.15 µg of drug was observed. The *in vivo* environment could induce the degradation of polymer due to the presence of enzymes and constant drenage of biological fluids. As a consequence, the leflunomide would be rapidly released from PCL implants and its controlled and sustained delivered could be compromised. However, as the biodegradation rate of polymer is extremely slow even in the biological environment, leflunomide was released by diffusion from polymeric implants. This fact explains the similarity between the *in vitro* and *in vivo* leflunomide release profiles.

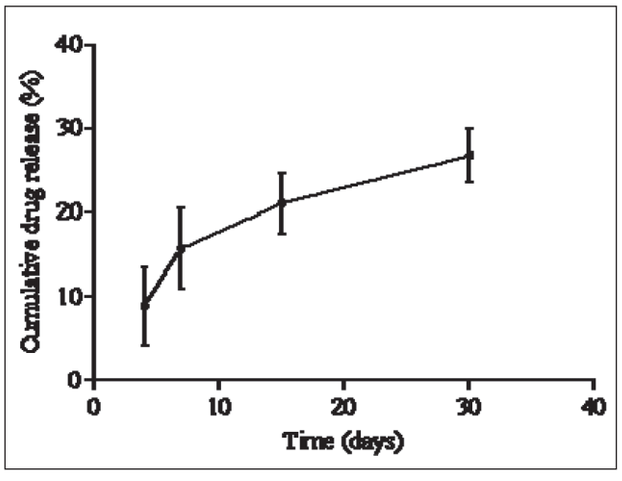

Fig. 8: Figure 8. In vivo cumulative release of leflunomide (%) from PCL implants. Results represent mean ± standard deviation (n = 5 for each day).

2.6. Murine sponge model

2.6.1. Measurement of MPO and NAG activities

At the moment of sponge implantation and tissue injury, platelets come into contact with exposed collagen and other elements of the extracellular matrix. This contact triggers the platelets to release clotting factors as well as essential growth factors and cytokines such as platelet-derived growth factor (PDGF) and transforming growth factor beta (TGF-beta). Following hemostasis, the neutrophils enter the wound site and begin the critical task of phagocytosis to remove foreign materials and damaged tissue (Diegelmann et al. 2005). In this study, the accumulation of activated neutrophils could be indirectly measured by assaying the MPO enzyme, which is specifically secreted by this cell population. It was verified that the MPO activity was attenuated by leflunomide released from PCL implants when compared to the MPO index of control group within 4, 7 and 10 days. Statistical analysis (one-way ANOVA) shows that there was a significant difference in the concentration of MPO in the sponge discs between the treated and untreated groups ($p < 0.05$) (Fig. 9A). The obtained results corroborated with those previously reported by Ozturk et al. (2008). In this report, leflunomide was capable of reducing the lung injury after cecal ligation puncture-induced sepsis by inhibition of neutrophils accumulation, demonstrated by the regression of MPO levels. Additionally, Karaman et al. (2006) described the significant attenuation of MPO activity after the administration of leflunomide in an experimental model of extrahepatic cholestasis. Therefore, the inflammation inhibiting effect of leflunomide delivered from PCL implants may reflect the reduction in the migration of neutrophils into the non-biocompatible sponge.

As part of the inflammatory phase, neutrophils and monocytes progressively migrate from the circulation to the injured tissue. Activated monocytes differentiate into macrophages. Macrophages appear and continue the process of phagocytosis as well as releasing more PDGF and TGF-beta. Subsequently, macrophage proliferation increases, attracting smooth muscle cells and fibroblasts to begin the proliferative phase and deposit new extracellular matrix (Diegelmann et al. 2005). The influence of leflunomide on activated macrophages was assessed by the measurement of NAG lysosomal enzymes that are specific for this cell population. Accordingly, NAG activity was not affected by the leflunomide released from the PCL implants after 7 days of sponge insertion. However, leflunomide downregulated significantly the NAG index at the 10th day after sponge implantation ($p > 0.05$) (Fig. 9B). Therefore, the leflunomide controlled delivered by PCL implants probably affected the recruitment of this inflammatory cell population just in a later phase of the injury. Consistent with this result was the finding that the systemic administration of teriflunomide at approximately 3 mg kg^{-1} per day caused a significant decrease in monocytes, and consequently macrophages, in arthritic rats after 10 days of treatment (Balagué et al. 2012). However, leflunomide PCL implants displayed a therapeutic effect with one single implantation; and the treatment with free teriflunomide required a daily administration of drug to regulate the recruitment of macrophages, representing a disadvantage of this conventional treatment. Additionally, the systemic administration of teriflunomide at approximately 10 mg kg^{-1} promoted extensive pancytopenia (leukocytopenia, thrombocytopenia and erythropenia) relative to the un-induced arthritis in rats (Balagué et al. 2012). This report demonstrated another disadvantage of the conventional pharmaceutical dosage forms, which affected stem cells causing intense myelosuppression. By contrast, PCL implants containing leflunomide could deliver therapeutic levels of drug directly into the targeted site, probably minimizing severe side effects frequently observed after systemic administration.

2.6.2. Measurement of nitric oxide (NO) content

Following activation, proinflammatory macrophages produce a large number of mediators and cytokines including interleukin-1, interleukin-6, interleukin-12, TNFα, and inducible nitric oxide synthase (iNOS) (Koh et al. 2011). However, many of these mediators have been shown to be present in the early wound environment, indicating that inflammatory cells such as neutrophils could be another source of iNOS production. NO production is directly involved in the pathogenesis of several autoimmune diseases such as rheumatoid arthritis and multiple sclerosis, inducing tissue destructive actions (Miljkovic et al. 2011). Then, the suppression of iNOS, and consequently, the NO levels, might partly account for the anti-inflammatory effects at the pathological site. In this study, it was verified that leflunomide released from PCL implants was capable of inducing significant regression of the NO index in the sponge discs. The NO accumulation in the sponges of the untreated group, which did not receive the leflunomide PCL implants, was remarkable. Leflunomide attenuated the excessive NO levels by suppressing iNOS, produced by different types of inflammatory cells such as neutrophils, in the early days of the experiment, and probably activated macrophages,

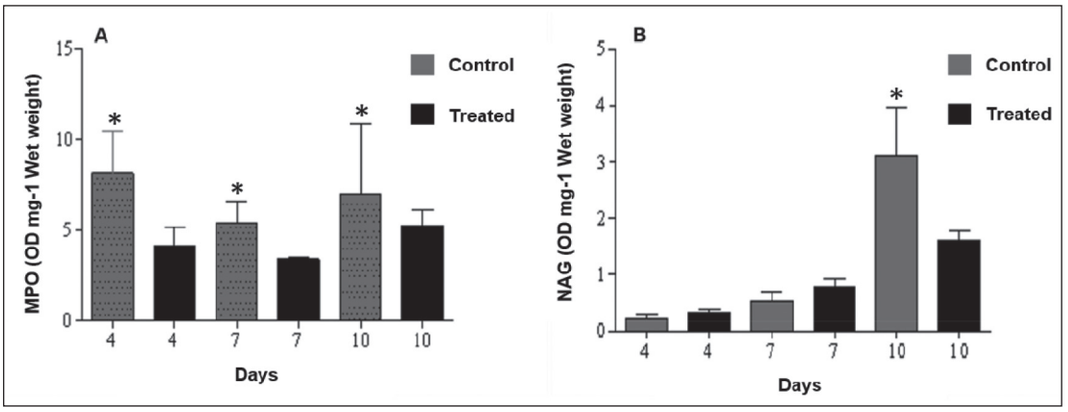

Fig. 9: Levels of neutrophil (A), and monocytes■macrophage (B) accumulation, measured by MPO and NAG activities, respectively, in the sponge matrices of treated group (sponges containing leflunomide PCL implants), and control group. Values represent means ■ SEM of 6 animals per group.

at 4, 7 and 10 days after sponge implantation. The statistical analysis (one-way ANOVA) demonstrated that the concentration of NO in both groups was significantly different ($p < 0.05$) (Fig. 10). These results corroborated with those previously reported by Milijovik et al. (2011) who have demonstrated the ability of the leflunomide to suppress the iNOS-mediated NO synthesis in astrocytes *in vitro*, which are implicated in inflammatory destruction of brain tissue, including those occurring in multiple sclerosis. Additionally, the alteration of the iNOS production by leflunomide in human beings has been demonstrated by Reddy et al. (2005). It was reported that the serum nitrite and citrulline levels after 4 weeks of treatment with leflunomide significantly decreased in patients with active rheumatoid arthritis. Therefore, leflunomide controlled delivered by polymeric implants inhibited the synthesis of NO in the inflamed site, and may represent one of the important mechanisms of pharmacological action of this anti-rheumatic drug.

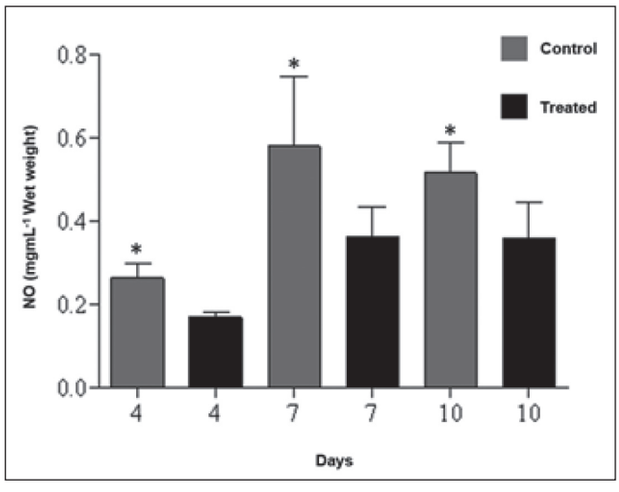

Fig. 10: Nitric oxide (NO) levels in sponge discs of treated group (sponges containing leflunomide PCL implants) (gray bar), and control group (black bar). Values represent means ■ SEM of 6 animals per group.

2.6.3. *Measurement of hemoglobin (Hb) content*

Inflammation and angiogenesis are key processes that act simultaneously and synergistically to maintain diseases (Da Silva et al. 2009). Angiogenesis is a complex and critical process that leads to the formation of new blood vessel from pre-existing ones (Koh et al. 2011). The angiogenic process is frequently driven by an excess of vascular endothelial growth factor (VEGF), NO, or other mediators produced by infiltrated macrophages, endothelial and NK cells. The resolution of the inflammation and the onset of lasting tissue repair cause the newly formed vasculature to regress, resulting in the restoration of homeostatic control. In the absence of vascular regression, positive feedback mechanisms operating between vessels and the inflammatory infiltrate sustain the new vasculature and further exacerbate the inflammatory response. This is the case in severe pathologies such as atherosclerosis, rheumatoid arthritis, and psoriasis (Arroyo et al. 2010; Mazzone et al. 2009). In this work, the extent of angiogenesis could be estimated by detecting the Hb content in the sponge discs. It was observed that the Hb index in the animals receiving leflunomide PCL implants was significantly lower than that obtained for the control group at all days of experimentation (one-way ANOVA, $p < 0.05$), indicating that the drug released from polymeric implants suppressed the growth of new blood vessels in the inflamed tissue (Fig. 11). As the neovascularization was inhibited, the released leflunomide contributed to the resolution of inflammatory response, and consequently, it facilitated the tissue repair. The antiangiogenic activity of leflunomide was also described by Nars et al. (2014), who demonstrated that this drug was capable of inhibiting the VEGF expression, making the antiangiogenic process evident.

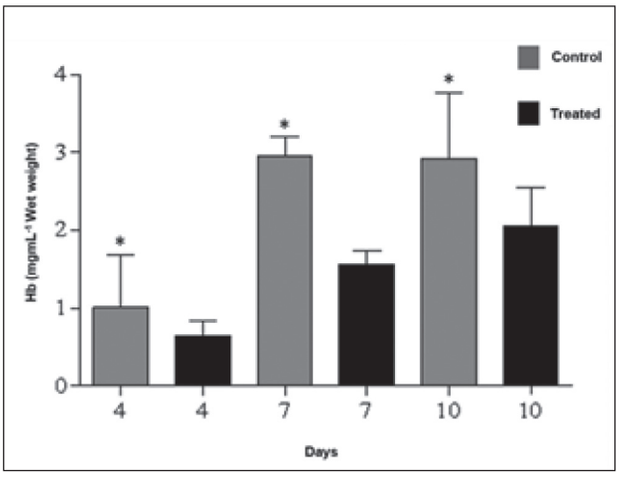

Fig. 11: Hemoglobin content in sponge discs of treated group (sponges containing leflunomide PCL implants) (gray bar), and control group (black bar). Values represent means ■ SEM of 6 animals per group.

2.6.4. *Histological examination*

The histological examination of sponge discs receiving leflunomide clearly demonstrated the inhibition of inflammatory and angiogenic responses, since the infiltration of inflammatory cells and the neovascularization were significantly decreased during the 10-day period of the experiment (Fig. 12). The qualitative histological findings corroborated with the measured biochemical parameters as described above.

2.7. *Toxicity*

To assess information about the toxicity of leflunomide PCL implants, kidneys and livers from animals under experimentation were collected

4, 7 and 10 days after implantion, and were analyzed by histological processing. The liver morphology of animals from control and treated groups showed no structural differences in the organization of hepato-

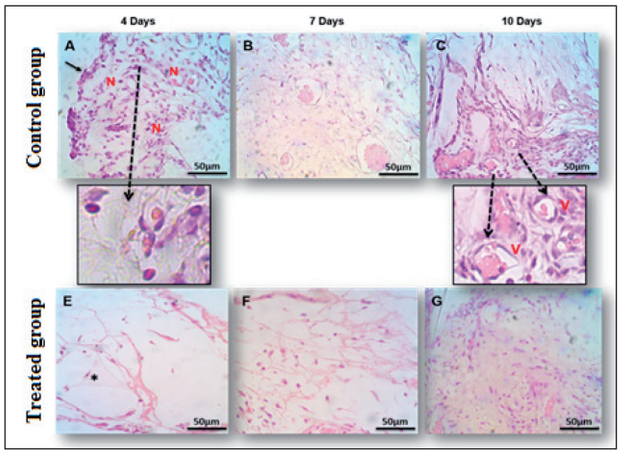

Fig. 12: Representative histological sections (5 µm, HE) of contrtol group (unloaded PCL implants) (A, B, C) and treated group (sponges containing leflunomide PCL implants) (D, E, F) after 4, 7 and 10 days post-sponge implantation, respectively. Photomicrographs represent the inflammatory infiltrate and angiogenesis during the period of the experiment. (*) Sponge trabecular. 50 µm bar = × 20 magnification. A, B, C (dashed arrow) - × 100 magnification. (V) New vessels. (N) Neutrophils.

cytes, ducts, vessels or arteries or star cells. Hepatocytes displayed a homogeneous cytoplasm, of polyhedral shape without degenerative alterations. The nucleus for the most part of hepatocytes exhibited an obvious nucleolus without signs of pycnotic formations. Signs of necrosis or connective changes of the extracellular matrix were not observed in any animal in both groups. Finally, hemorrhage and/or inflammatory infiltrate was not detected (Fig. 13).Therefore, leflunomide did not induce hepatotoxicity, since this drug was only locally released. By contrast, it has been previously shown, that leflunomide administrated by oral or parenteral routes, and systemically distributed, induced fatal hepatitis and liver failure (Ma et al. 2016).

The kidney morphology of animals from control and treated groups was also assessed, and glomeruli exhibited no changes. In addition, the existence of glomerulonephritis, degeneration and/or intratubular hyaline cylinders, which are indicative of nephrotoxicity, was not identifyed (Fig. 14). Therefore, leflunomide controlled delivered by polymeric implants did not cause injuries in the renal tissues.

2.8. Conclusion

In conclusion, leflunomide PCL implants were developed by melting the polymer and agglomerating the particles of drug. To quantify the leflunomide incorporated in implantable devices and released from them, a spectrophotometric method was developed and validated

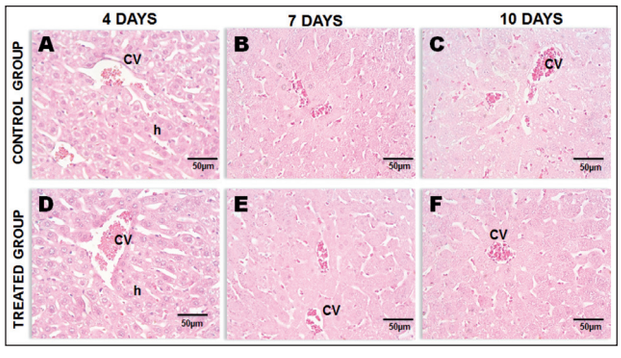

Fig. 13: Histological photomicrographs (4 mm, HE) of liver collected after 4, 7 and 10 days post implantation of leflunomide PCL implants. Photomicrographs in (A), (B) and (C) represented the hepatic tissues of animals from control group. Photomicrographs in (D), (E) and (F) represented the hepatic tissues of animals from treated group (receiving leflunomide PCL implants) (n = 5 - 6 mice per each time). CV, central vein. Bar = 50 µm.

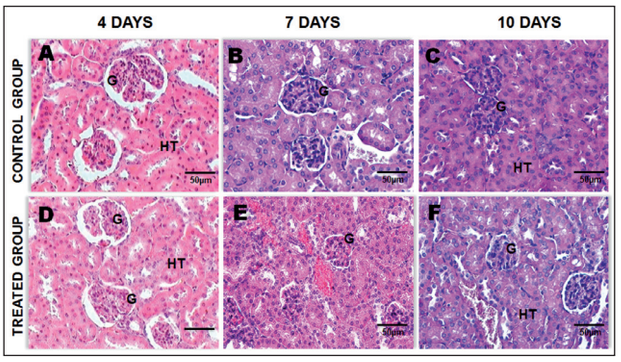

Fig. 14: Histological photomicrographs (4 mm, HE) of kidney collected after 4, 7 and 10 days post implantation of leflunomide PCL implants. Photomicrographs in (A), (B) and (C) represented the renal tissues of animals from control group. Photomicrographs in (D), (E) and (F) represented the hepatic tissues of animals from treated group (receiving leflunomide PCL implants) (n = 5 - 6 mice per each time). G = glomerulus; HT = hepatic tissue. Bar = 50 µm.

in terms of linearity, matrix effect, quantitation limit, precision, and accuracy. This method provided unequivocal quantitation of leflunomide, showing that the selected analytical conditions were suitable to avoid the interferenc of PCL in the assay of drug. Besides the uniform distribution of leflunomide into polymeric implants, the drug was completely dispersed in the matrix and showed chemical integrity. Leflunomide was delivered from PCL implants in a controlled and sustained way by a diffusion mechanism, providing the regression/inhibition of inflammatory angiogenesis triggered by the non-biocompatible sponge. In this context, neutrophil and monocyte/macrophage influx was attenuated due to the modulation of MPO and NAG activities, respectively. As the number of these pro-inflammatory cells was reduced, NO levels were also down-regulated, inducing an anti-inflammatory effect in the pathological site. Finally, considering the regression of inflammation, the Hb concentration in sponges was reduced drastically, indicanting that the descontruction of inflammatory process by leflunomide does not demand the formation of new vessels. In addition, the accumulation of leflunomide directly in the affected area avoided systemic adverse effects like hepatotoxicity and nephrotoxicity.In conclusion, the attenuation of inflammation and angiogenesis by leflunomide controlled released from PCL implants directly into the target tissue indicated the potential of these systems to act as intra-articular drug delivery implantable devices to treat synovitis in rheumatoid arthritis pacients without triggering systemic damages.

3. Experimental

3.1. Development of leflunomide PCL implants

Poly(ε-caprolactone) (PCL, MW ~ 14,000, Sigma Aldrich, USA) (20 mg) and leflunomide (Purifarma, Brazil) (80 mg) were dissolved in acetonitrile (9 mL). This solution was homogeinized for 15 min in an ultrasonic bath; and remained in the desiccator for 48 h to enable solvent evaporation. Blend was molded into spherical implants using a metallic mold at approximately 60-70 °C. Leflunomide-loaded PCL implants contained 2 mg of drug and 8 mg of polymer. Unloaded PCL implants were also developed. Implants were desinfected by exposure to ultraviolet light for 20 min.

3.2. Development and validation of spectrophotometric method to quantify leflunomide into PCL implants

3.2.1. Instrumentation and analytical conditions

A Shimadzu model 1700 (Japan) double beam UV/Visible spectrophotometer with spectral width of 2 nm, wavelength accuracy of 0.5 nm and a pair of 10 mm matched quartz cell was used to measure absorbance of all solutions. Spectra were automatically obtained by UV-Probe system software. The detection of leflunomide was carried out at 259 nm. Acetonitrile was used as analytical blank. All solutions were prepared in acetonitrile by using leflunomide reference standard.

3.2.2. Method validation

The spectrophotometric method was validated by determining the following parameters: linearity and matrix effect, precision, accuracy, and quantitation limit.

3.2.2.1. Linearity and matrix effect

Calibration curves were obtained using six drug reference standard concentrations (2.5; 5.0; 7.5; 10.0; 12.5 and 15.0 µg mL^{-1}) in 3 independent replicates run in random order. To verify the matrix effect, calibration curves were plotted using six drug reference standard concentrations (2.5; 5.0; 7.5; 10.0; 12.5 and 15.0 µgmL^{-1}) associated with PCL at the concentration of 15 µg mL^{-1} in 3 independent replicates run in random order. Linear regression analysis was done by the ordinal least squares method (OLSM). Residue analysis was performed (Meyer et al. 1993), and outliers were deleted by using the Jacknife standardized residual test (Belsley et al. 1980). Maximum exclusion of 22.2 % of original points was considered (Horwitz 1995). Then, normality by Ryan-Joiner test (Ryan 1996), homoscedasticity by Brown-Forsythe test (Levene 1960; Brown et al. 1970) and independency by Durbin-Watson test (Horwitz 1995) were achieved. For this model assumption, the lack-of-fit test (ANOVA) ($p > 0.05$), and the significance of regression ($p > 0.05$) were considered. Finally, as the linear model was suitable, slope and intercept were calculated to establish the equation that describes each calibration curve (calibration curve for leflunomide and calibration curve for leflunomide associated with PCL – matrix effect). Then, these calibration curves were compared by t-Student test assuming combined or distinct variances (Souza et al. 2005).

3.2.2.2. Quantitation limit

The limit of quantitation value (LOQ) is defined as the lowest concentration that can be quantitatively determined with suitable precision and accuracy. The LOQ was calculated directly from the calibration curve and can be expressed as:

$$LOQ = \frac{10\sigma}{b} \qquad (1)$$

where, σ is the standard deviation of the response and b is the slope of the calibration curve.

3.2.2.3. Precision

Precision was determined based on repeatability and intermediate precision. Repeatability was assessed through the assay of solutions at concentrations of 5.0; 10.0; and 15.0 µg mL^{-1} on the same day. The solutions were prepared in triplicate with leflunomide associated with PCL at the concentration of 15 µg mL^{-1}. Intermediate precision was verified by evaluating the results on 3 different days. Precision was expressed as coefficient of variation (CV) amongst responses.

3.2.2.4. Accuracy

To determine accuracy, standard solutions at concentrations of 5.0; 10.0 and 15.0 µg mL^{-1} were prepared in triplicate with leflunomide associated with PCL at the concentration of 15 µg mL^{-1}. The solutions were assayed on three different days (n = 18 for each concentration). The percent recovery of added leflunomide was calculated comparing absorvances of resultant solutions with leflunomide standard solutions at the same concentration. The relative error was also calculated.

3.3. Determination of leflunomide content incorporated into PCL implants

Ten implants were selected and weighted (n = 10). Each implant was dissolved in acetonitrile to obtain a solution at 10 µg mL^{-1} of leflunomide. The amount of drug in each implant was quantified with the spectrophotometric method previously developed and validated. The uniformity content of leflunomide was expressed as the percent of the pre-indicated value (approximately 2.0 mg). The relative standard deviation was also calculated.

3.4. Characterization

Infrared spectra were collected in a Fourier Transform Infrared Spectrophotometer (FTIR; Perkin Elmer, model Spectrum 1000). Measurements were carried out using the Attenuated Total Reflectance (ATR) technique. Each spectrum was a result of 32 scans with a resolution of 4 cm^{-1}.

Differential scanning calorimetric (DSC) thermograms were obtained on a Mettler Toledo DSC (Switzerland). Samples were put into aluminium pans. The calorimeter was calibrated for temperature and heat flow accuracy using pure indium melting (m.p. 156.6 °C and DH = 25.45 J g^{-1}). The temperature ranged from 25-300 °C with a heating rate of 25 °C min^{-1} under nitrogen atmosphere.

3.5. In vitro release of leflunomide from PCL implants

In vitro release of leflunomide was carried out during 90 days. Leflunomide- PCL implants were immersed in different tubes containing 71 mL of phosphate buffer solution (PBS, pH = 7.4) (n = 5). These tubes were incubated at 37 ºC and 40 rpm. At predetermined intervals (0, 4, 7, 15, 30, 45, 60, 75 and 90 days), the release medium was collected, and completely renewed with fresh PBS. The amount of leflunomide released from each implant was quantified by using the spectrophotometric method previously developed and validated. The release profile was evaluated as the cumulative percentage of drug delivered in the medium.

3.6. In vivo release of leflunomide from PCL implants

3.6.1. Animals

Six to eight weeks old female Swiss mice from the Federal University of Ouro Preto were maintained in individual cases, with food and water *ad libitum*, and controlled temperature and humidity in the animal house of the Federal University of Ouro Preto. Experiments were approved by the Ethics Committee in Animal Experimentation at Federal University of Ouro Preto.

Animals were anesthetized with a mixture of 10 mg kg^{-1} of xylazine and 100 mg kg^{-1} of ketamine hydrochloride (i.p.). Their dorsal hair was shaved and the skin wiped with 70 % (v v^{-1}) ethanol. Leflunomide PCL implants were aseptically inserted into a subcutaneous pouch that had been made with curved artery forceps through a 1 cm long dorsal mid-line incision. After the implantation procedure, the animals were maintained in individual cages and provided with chow pellets and water *ad libitum*. The light/dark cycle was 12:12 h with lights on at 7:00 am and lights off at 7:00 pm. At 4, 7, 15, and 30 days after implantation, animals (n = 5 for each time) were euthanized, and implants were carefully removed. The implant was fragmented using a scissor, and pieces were dissolved in 10 mL of acetonitrile. The content of leflunomide remaining in the PCL implants was measured using the validated spectrophotometric method.

3.7. Murine sponge model

3.7.1. Preparation of sponge discs

Animals described under 2.6.1 were used in the murine sponge model. Non-biocompatible polymeric sponge discs (5 mm in thickness, 8 mm in diameter, and approximately 4.6 mg in weight) (Vitaform Ltd, Manchester, UK) were used as the matrix for fibrovascular tissue growth. Sponge discs were soaked overnight in a 70 % (V V^{-1}) ethanol solution and sterilized by boiling in distilled water for 15 min before the implantation surgery.

3.7.2. Implantation of sponge discs and leflunomide-loaded PCL implants

Animals were anesthetized with a mixture of xylazine (10 mg kg^{-1}) and ketamine hydrochloride (100 mg kg^{-1}) (i.p.). Their dorsal hair was shaved, and the skin wiped with 70 % (V V^{-1}) ethanol. Leflunomide PCL implants were incorporated into the sponge discs, and they were aseptically inserted into a subcutaneous pouch that had been made with curved artery forceps through a 1 cm long dorsal mid-line incision (treated group). The same implantation procedure was carried out in order to insert the sponge discs containing unloaded implants (control group). Post-operatively, animals were monitored for any signs of infection at the operative site, or upon discomfort or distress; any mice presenting such signs were immediately sacrificed.

3.7.3. Measurement of hemoglobin (Hb) content

The extent of vascularization of sponge discs was assessed by the amount of Hb detected in the tissue using the Drabkin method (Drabkin et al. 1932). At 4, 7 and 10 days post-implantation, six animals of treated and control groups were euthanized and the sponge discs were carefully removed. Sponges were dissected from adherent tissue, weighed, homogenized in 2 mL of Drabkin reagent (Labtest, São Paulo, Brazil) and centrifuged at 4 °C at 12.000 *g* for 20 min. Supernatants were filtered through a 0.22 µm Millipore filter. The Hb concentration of samples was determined by measuring the absorbance at 540 nm using an ELISA plate reader, and was compared against a standard curve of Hb. The content of Hb in the sponge discs was expressed as micrograms of Hb per milligram of wet tissue.

3.7.4. Tissue extraction and determination of myeloperoxidase (MPO) and N-acetyl-β-d-glucosaminidase (NAG) activities

The extent of neutrophil accumulation in the sponge discs was measured by assaying MPO activity (Bradley et al. 1982). After processing the supernatant of sponges (n = 6 for each group) for Hb determination, a part of the corresponding sponge was weighed, homogenized in 2 mL of buffer pH 4.7 (0.1 mol L^{-1} NaCl, 0.02 mol L^{-1} Na_2PO_4, 0.015 mol L^{-1} Na_2-EDTA), and centrifuged at 4 °C at 12.000 *g* for 10 mins. Sponges were then re-suspended in a 0.05 mol L^{-1} sodium phosphate buffer (pH 5.4) containing 0.5 % hexa-1,6-*bis*-decyl trimethyl ammonium bromide (HTAB). MPO activity in the supernatant samples was assayed by measuring the change in absorbance (optical density; OD) at 450 nm using 3,3'-5,5'-tetramethylbenzidine (TMB) prepared in dimethyl sulfoxide (DMSO) at a final concentration of 1.6 mM and H_2O_2 (0.3 mM) in the sodium phosphate buffer, pH 6.0.The reaction was terminated by the addition of 50 µL of H_2SO_4 (4 mol L^{-1}). Results were expressed as change in OD per milligram of wet tissue (Silva-Filho et al. 2012).

The infiltration of mononuclear cells into the sponge discs was quantified by measuring the levels of the lysosomal enzyme *N*-acetyl-β-d-glucosaminidase (NAG) which is present in high levels in activated macrophages (Bradley et al. 1982; Belo et al. 2004). A portion of sponges that remained after the Hb measurement was kept for this assay (n = 6 for each group). These sponges were weighed, homogenized in a NaCl solution 0.9 % (W V^{-1}) containing 0.1 % (V V^{-1}) Triton X-100 (Promega), and centrifuged (3000 *g*; 10 min at 4 °C). Samples of the resulting supernatant (100 µL) were incubated for 10 min with 100 µL *p*-nitrophenyl-*N*-acetyl-β-d-glucosaminide (Sigma-Aldrich) prepared in the citrate/sodium phosphate buffer (0.1 mol L^{-1} citric acid, 0.1 mol L^{-1} Na_2HPO_4; pH 4.5) to yield a final concentration of 2.24 mM. The reaction was stopped by the addition of 100 µL of 0.2 mol L^{-1} glycine buffer (pH 10.6). Hydrolysis of the substrate was determined by measuring the absorption at 400 nm. NAG activity was expressed as the change in OD per milligram of wet tissue (Silva-Filho et al. 2012).

3.7.5. Measurement of nitric oxide (NO) content

Basal production of nitric oxide (NO) by sponge discs was measured in the perfusate using carbon micro sensors with a NO permeable membrane (ISO-NOPF100; World Precision Instruments Inc., Sarasota, FL, USA). Carbon micro sensors to NO were stabilized for 1 h in Krebs buffer solution (in mM): 110.8 NaCl, 5.9 KCl, 25.0 $NaHCO_3$, 1.07 $MgSO_4$, 2.49 $CaCl_2$, 2.33 NaH_2PO_4 and 11.51 glucose, pH 7.4. At day 4, 7 and 10 after implantation, six animals of treated and control groups were euthanized and the sponge discs were carefully removed and rinsed in 50 mL of

Krebs buffer solution, stood for 5 min, and then placed in 1.5 mL of gassed (95 % O_2 and 5 % CO_2) Krebs solution, at 37 °C. Carbon micro sensors were connected to an amplifier-recorder (TBR-4100 Free Radical Analyzer; World Precision Instruments Inc.) and to a computer equipped with a data acquisition board (Lab-Trax-4/16; World Precision Instruments Inc.), using Lab-Trax software (World Precision Instruments Inc.). Currents (nA) were measured by micro sensors continuously (30 minutes) and NO concentrations were determined by calibrations curves of known concentrations of *S*-nitroso-*N*-acetyl-dl-penicillamine (SNAP; 0.2-500 nM) (Araújo et al. 2013).

3.7.6. Histological examination

Animals were anesthetized and euthanized by cervical dislocation 4, 7, and 10 days after implantation. Adjacent tissues to the sponge discs were carefully collected and fixed in formalin [10 % (V V^{-1}) in isotonic saline] for 48 h. Tissues were embedded in paraffin and 5 µm thick sections were obtained. Sections were stained with hematoxylin and eosin and examined under an objective 40 × lens in light microscopy. Images were digitized through a microcamera JVC-TK1270/JG Band transferred to an image analyzer (KS300 version 2; Kontron Electronics, Carl Zeiss).

3.8. Toxicity

Sponge discs, liver, and kidney tissues of each mouse under experimentation were fixed in 10 % (V V^{-1}) buffered formaldehyde pH 7.4 for at least 48 h. Fragments of the sponge and organs, measuring approximately 1 cm^2, were included in 60 % (W V^{-1}) paraffin. Sections (4 mm) were obtained and stained by hematoxylin-eosin. Images were digitalized through a microcamera (JVC-TK 1270/JGB) and transferred to an analyzer (Kontron Electronics, Carls Zeiss-KS300 version 2) (De Oliveira et al. 2015).

3.9. Statistical analysis

Results were expressed as mean ± standard deviation. Data were tested for normality and investigated for statistical significance using one-way analysis of variance (ANOVA). A *P*-value of less than 0.05 was considered statistically significant. Statistical analysis was performed using a Graph-Pad Prim 5.

Acknowledments: The authors would like to acknowledge the financial support received from the following institutions: CNPq/MCT (Brazil), FAPEMIG (Minas Gerais – Brazil), UFOP (Minas Gerais – Brazil) and UFSJ (Minas Gerais – Brazil).

Statements: The authors declare that the research data used in preparation of the manuscript is available with G.R. Da Silva and T.F. Gomes.

Conflicts of interest: The authors declare that there is no conflict of interest regarding the publication of this paper.

References

Alén JC, Pérez T, Yuste SR, Ferraz-Amaro I, Alegre JJS, Pinto JAT, Pan MF, Quevedo JC, Hernández-Hernández MV, Hidalgo CC, San Martín, AA, Sánchez MIT, Sanmartí R (2018) Efficacy and safety of combined therapy with synthetic disease-modifying antirheumatic drugs in rheumatoid arthritis: systematic literature review. Reumatol Clin. 18, pii: S1699-258X(18)30175-X.

Araújo FA, Rocha MA, Capettini LS, Campos PP, Ferreira MA, Lemos VS, Andrade SP (2013) 3-Hydroxy-3-methylglutaryl coenzyme A reductase inhibitor (fluvastatin) decreases inflammatory angiogenesis in mice. APMIS 121: 422 – 430.

Arroyo AG, Iruela-Arispe ML (2010) Extracellular matrix, inflammation, and the angiogenic response. Cardiovasc Res 86: 226 - 235.

Balagué C, Pont M, Prats N, Godessart N (2012) Profiling of dihydroorotate dehydrogenase, p38 and JAK inhibitors in the rat adjuvant-induced arthritis model: a translational study. Br J Pharmacol 166: 1320 - 1332.

Bastian H, Feist E, Burmester GR (2011) Therapeutic strategies in rheumatoid arthritis. Internist 52: 645 – 656.

Belo AV, Barcelos LS, Teixeira MM, Ferreira MAND, Andrade SP (2004) Differential effects of antiangiogenic compounds in neovascularization, leukocyte recruitment, VEGF production, and tumor growth in mice. Cancer Invest 22: 723 - 729.

Belsley DA, Kuh E, Welsch RE (1980) Regression diagnostics: identifying influential data and sources of collinearity, Wiley, New York.

Bongartz T, Sutton AJ, Sweeting MJ, Buchan I, Matteson EL, Montori V (2006) Anti-TNF antibody therapy in rheumatoid arthritis and the risk of serious infections and malignancies: systematic review and meta-analysis of rare harmful effects in randomized controlled trials. JAMA 295: 2275 - 2285.

Boone NW, Teeuwisse P, Van Der Kuy PH, Janknegt R, Landewé RBM (2015) Evaluating patient reported outcomes in routine practice of patients with rheumatoid arthritis treated with biological disease modifying anti rheumatic drugs (b-DMARDs), Springer plus. 4.

Bradley PP, Priebat DA, Christensen RD, Rothstein G (1982) Measurement of cutaneous inflammation: estimation of neutrophil content with an enzyme marker. J Invest Dermatol 78: 206 -209.

Brown MB, Forsythe AB (1974) Robust tests for the equality of variances. JASA 69: 364 - 367.

Cheng L, Guo S, Wu W (2009) Characterization and in vitro release of praziquantel from poly(epsilon-caprolactone) implants. Int J Pharm 377: 112 - 119.

Da Silva GR, Ayres E, Oréfice RL, Moura SAL, Cara DC, Silva-Cunha A (2009) Controlled release of dexamethasone acetate from biodegradable and biocompatible polyurethane and polyurethane nanocomposite, Drug Target 17: 374 - 383.

Day MJ (2008) Immunomodulatory therapy. In: Small Animal Clinical Pharmacology. 2° ed. Elsevier, pp. 270 – 286.

De Oliveira LG, De Miranda MB, De Moura SAL, De Miranda MB, Da Silva GR (2018) Tacrolimus delivered from polymeric implants suppressed inflammation and angiogenesis in vivo without inducing nephrotoxicity, hepatotoxicity, and myelosuppression. J Drug Deliver Sci Technol 43: 487 - 495.

De Oliveira LG, Figueiredo LA, Fernandes-Cunha GM, De Miranda MB, Machado LA, Da Silva GR, Moura SAL (2015) Methotrexate locally released from poly(ε-caprolactone) implants: inhibition of the inflammatory angiogenesis response in a murine sponge model and absence of systemic toxicity. J Pharm Sci 104: 3731 - 3742.

Diegelmann RF, Evans MC (2004) Wound healing: an overview of acute, fibrotic and delayed healing, Front Biosci. 9 283 - 289.

Drabkin DL, Austin JH (1932) Spectrophotometric studies: i. spectrophotometric constants for common hemoglobin derivatives in human, dog, and rabbit blood. J Biol Chem 98: 719.

Durbin J, Watson GS (1951) Testing for serial correlation in least squares regression, Biometrika 38: 159 - 178.

Hernádez MHG, Amaro RG, Pérez DPP (2014) Specific therapy to regulate inflammation in rheumatoid arthritis: molecular aspects. Future Med J 6: 623 - 636.

Horwitz W (1995) Protocol for the design, conduct and interpretation of method-performance studies: Revised 1994 (Technical Report), Pure Applied Chem 67: 331 - 343.

Karaman A, Iraz M, Kirimlioglu H, Karadag N, Tas E, Fadillioglu E (2006) Hepatic damage in biliary-obstructed rats is ameliorated by leflunomide treatment. Pediatr Surg Int 22: 701 – 708.

Koh TJ, Dipietro LA (2011) Inflammation and wound healing: the role of the macrophage. Expert Rev Mol Med 11: e23.

Levene H (1960) in: Olkin I, Ghurye SG, Hoeffding W, Madow WG, Mann HB. eds. Contributions to probability and statistics:, Stanford University Press, Stanford.

Ma LL, Wu ZT, Wang L, Zhang XF, Wang J, Chen C, Ni X, Lin YF, Cao YY, Luan Y, Pan GY (2016) Inhibition of hepatic cytochrome P450 enzymes and sodium/bile acid cotransporter exacerbates leflunomide-induced hepatotoxicity. Acta Pharmacol Sin 37: 415 - 424.

Mazzone M, Dettorim D, De Oliveira RL, Loges S, Schmidt T, Jonckx B, Tian YM, Lanahan AA, Pollard P, Almodovar CR, De Smet F, Vinckier S, Aragonés J, Debackere K, Luttun A, Wyns S, Jordan B, Pisacane A, Gallez B, Lampugnani MG, Dejana E, Simons M, Ratcliffe P, Maxwell P, Carmeliet P (2009) Heterozygous deficiency of PHD2 restores tumor oxygenation and inhibits metastasis via endothelial normalization. Cell 136: 839 - 851.

Mccauley JA, Brittain HG (2005) Thermal method of analysis, in: H.G. Brittain (ed.): Physical Characterization of Pharmaceutical Solids, Drugs and Pharmaceutical Sciences, Marcel Dekker Inc, New York, pp. 223 – 250.

Mcinnes IB, O'Dell JR (2010) State-of-the-art: rheumatoid arthritis. Ann Rheum Dis 69: 1898 - 1906.

Meyer PC, Zund RE (1993) Statistical methods in analytical chemistry, John Wiley & Sons, New York.

Miljkovic D, Samardzic T, Mostarica SM, Stosic-Grujicic S, Popadic D, Trajkovic V (2011) Leflunomide inhibits activation of inducible nitric oxide synthase in rat astrocytes. Brain Res 889: 331 - 338.

Moura SAL, Lima LDC, Andrade SP, Silva-Cunha A, Oréfice RL, Ayres E, Da Silva GR (2011) Local drug delivery system: inhibition of inflammatory angiogenesis in a murine sponge model by dexamethasone-loaded polyurethane implants. J Pharm Sci 100: 2886 – 2895.

Nasr M, Selima E, Hamed O, Kazem A (2014) Targeting different angiogenic pathways with combination of curcumin, leflunomide and perindopril inhibits diethylnitrosamine-induced hepatocellular carcinoma in mice, Eur J Pharmacol 15: 267 - 275.

Orellano LA, Almeida SA, Campos PP, Andrade SP (2015) Angiopreventive versus angiopromoting effects of allopurinol in the murine sponge model. Microvasc Res 101: 118 - 126.

Ozturk, Demirbilek S, Begec Z, Surucu M, Fadillioglu E, Kirimlioglu H, Ersoy (2008) Does leflunomide attenuate the sepsis-induced acute lung injury? Pediatr Surg Int 24: 899 – 905.

Reddy SVB, Wanchu A, Khullar M, Govindrajan S, Bambery P (2005) Leflunomide reduces nitric oxide production in patients with active rheumatoid arthritis. Int Immunopharmacol 5: 1085 - 1090.

Rubinstein I, Weinberg GL (2012) Nanomedicines for chronic non-infectious arthritis: the clinician's perspective. Maturitas 8: 77 - 88.

Ryan TA, Joiner BL (1976) Normal probability plots and tests for normality, The State College, Pennsylvania State University.

Scott DL, Wolfe F, Huizinga TW (2010) Rheumatoid arthritis. Lancet 376: 1094 – 1108.

Siafaka PI, Barmbalexis P, Bikiaris DN (2016) Novel electrospun nanofibrous matrices prepared from poly (lactic acid)/poly(butylene adipate) blends for controlled release formulations of an anti-rheumatoid agent, Eur J Pharm Sci 88: 12 - 25.

Silva AFO, Castro WV, Andrade FP (2018) Development of spectrophotometric method for iron in fortified wheat and maize flours. Food Chem 242: 205 – 210.

Silva-Filho AL, Belo AV, Lages EL, Lamaita RM, Carneiro MM, Andrade SP (2012) Distinct pattern of inflammatory enzyme activities in human ovarian cancer and benign myoma. J Anal Oncol 1: 129 - 134.

Solano AG, Pereira AF, Pinto FC, Ferreira LG, Barbosa LAO, Fialho SL, Oliveira PPS, Silva-Cunha A, Da Silva GR, Pianetti GA (2013) Development and evaluation of sustained-release etoposide-loaded poly(ε-caprolactone) implants. AAPS PharmSciTech 14: 890 - 900.

Souza SVC, Junqueira RG (2005) Aprocedure to assess linearity by ordinary least squares method. Anal Chim Acta 552: 25 – 35.

U.S. FDA Drug Safety Communication: New boxed warning for severe liver injury with arthritis drug Arava (leflunomide). 2010.

Vega D, Petragalli A, Fernandez D, Ellena JA (2006) Polymorphism on leflunomide: stability and crystal structures. J Pharm Sci 95: 1075 – 1083.

Xuan J, Ren Z, Qing T, Couch L, Shi L, Tolleson WH, Guo L (2018) Mitochondrial dysfunction induced by leflunomide and its active metabolite. Toxicol. 8: 396 - 397.